Fluorescent Carbon Nanoparticle-Based Lateral Flow Biosensor for Ultrasensitive Detection of DNA

Sunitha Takalkar, Kwaku Baryeh, Guodong Liu

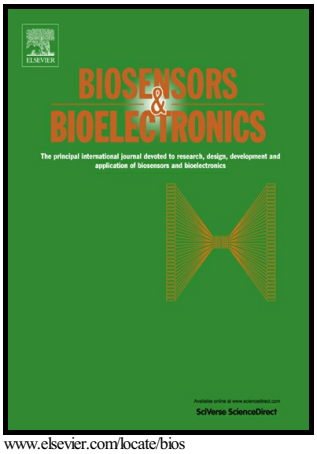

www.elsevier.com/locate/bios

PII: S0956-5663(17)30420-7
DOI: http://dx.doi.org/10.1016/j.bios.2017.06.045
Reference: BIOS9815

To appear in: *Biosensors and Bioelectronic*

Received date: 26 April 2017
Revised date: 6 June 2017
Accepted date: 21 June 2017

Cite this article as: Sunitha Takalkar, Kwaku Baryeh and Guodong Liu Fluorescent Carbon Nanoparticle-Based Lateral Flow Biosensor fo Ultrasensitive Detection of DNA, *Biosensors and Bioelectronic* http://dx.doi.org/10.1016/j.bios.2017.06.045

Fluorescent Carbon Nanoparticle-Based Lateral Flow Biosensor for Ultrasensitive Detection of DNA

Sunitha Takalkar, Kwaku Baryeh, Guodong Liu*

Department of Chemistry and Biochemistry, North Dakota State University, Fargo, ND, 58102

Abstract

We report a fluorescent carbon nanoparticle (FCN)-based lateral flow biosensor for ultrasensitive detection of DNA. Fluorescent carbon nanoparticle with a diameter of around 15 nm was used as a tag to label a detection DNA probe, which was complementary with the part of target DNA. A capture DNA probe was immobilized on the test zone of the lateral flow biosensor. Sandwich-type hybridization reactions among the FCN-labeled DNA probe, target DNA and capture DNA probe were performed on the lateral flow biosensor. In the presence of target DNA, FCNs were captured on the test zone of the biosensor and the fluorescent intensity of the captured FCNs was measured with a portable fluorescent reader. After systematic optimizations of experimental parameters (the components of running buffers, the concentration of detection DNA probe used in the preparation of FCN-DNA conjugates, the amount of FCN-DNA dispensed on the conjugate pad and the dispensing cycles of the capture DNA probes on the test-zone), the biosensor could detect a minimum concentration of 0.4 fM DNA. This study provides a rapid and low-cost approach for DNA detection with high sensitivity, showing great promise for clinical application and biomedical diagnosis.

Keywords: Fluorescent Carbon Nanoparticle, Lateral flow biosensor, DNA,

**Correspondence Author. Tel.: +1 701 231 8697; fax: +1 701 231 8831.*

E-mail: guodong.liu@ndsu.edu (G. Liu)

1. INTRODUCTION

In the field of molecular diagnostics, there exists an urgent need for the development of ultrasensitive tools for the detection of nucleic acids and proteins with high sensitivity and low cost (Shipp, 2006). Lateral flow strip biosensor, also called immunochromatography strip test, that combines the optical properties of colloidal gold with conventional immunoassay has attracted significant attention in biological analysis and clinical diagnosis (Weller., 2000, Sajid et al., 2015 and Ge et al., 2014). Recently the lateral flow device has been used to develop nucleic acid biosensors for qualitative (visual) or quantitative detection of nucleic acids (Mao et al., 2009 and He et al., 2010), protein biomarkers (Xu et al., 2009), cancer cells (Liu et al., 2009) and heavy metal ions (He et al., 2011) at low cost. Gold nano particles (GNP) were used as a colored tag and the produced red bands on the test zone of the device were detected by naked-eye for visual detection, or a portable strip reader for quantitative analysis. (He et al., 2010, 2011, Liu et al., 2009, Mao et al., 2009 and Xu et al., 2009). One of the drawbacks of the GNP-based lateral flow nucleic acid biosensors (LFNAB) is low sensitivity, which limits the applications in detecting very low concentrations of targets. Great effort has been applied to enhance the sensitivity of the LFNABs. Carbon nanotubes (Qiu et al., 2015), GNP-coated silica nanorods (Xu et al., 2014) and horseradish peroxidase (HRP)-coated GNP (He et al., 2011) have been used as colored tags to improve the sensitivities of the LFNAB. The LFNAB integrated with conventional nucleic acid amplification techniques including PCR (Polymerase Chain Reaction) (Mens et al., 2012 and Ang et al., 2012), isothermal amplification (Carter and Cary., 2007, Jaroenram et al., 2009, He et al., 2010) and other signal amplification techniques (Liu et al., 2013 and Lie et al., 2012) have shown a great enhancement of the sensitivities of LFNABs, however

complex operations and the use of many reagents offset the part of the advantages of the lateral flow biosensors.

Fluorescent nanoparticles are a great alternative to counterfeit the problems of sensitivity associated with colorimetric detections (Zheng et al., 2012 and Kim et al., 2011), Quantum dots (Li et al., 2010), fluorophore-labeled sequences (Xu et al., 2014), dye-doped silica nanoparticles (Wang and Nugen., 2013) and up-converting phosphor reporters (Corstjens et al., 2003) have been used as fluorescent tags to prepare the fluorescent lateral flow biosensors for ultrasensitive detection of nucleic acid sequences. The sensitivities of the fluorescent lateral flow nucleic acid biosensors without additional signal amplification were 1-3 orders higher than that of GNP-based colorimetric lateral flow biosensors. Despite the high sensitivities of fluorescent lateral flow nucleic acid biosensors, there are some drawbacks such as toxicity, complexity in synthesis of quantum dots and dye-doped silica nanoparticles, photo bleaching of the dye labelled sequences, defects in doping of the dye into nanoparticles. In light of all these problems, we have developed a fluorescent carbon nanoparticle (FCN)-based lateral flow biosensor for ultrasensitive detection of DNA sequences using a relatively simple, easy, and green synthetic procedure. FCNs as a new kind of fluorescent nanoparticles have recently attracted considerable research interests in a wide range of applications due to their low-cost and good biocompatibility (Fang et al., 2012). FCNs have been used in bio imaging (Cao et al., 2007 and Yang et al., 2009), photo catalysis (Li et al., 2010 and Cao et al., 2011), light emitting devices (Wang et al., 2011), biosensors (Dai et al., 2014 and Wang et al., 2011) and fluorescent detection of metal ions (Cui et al., 2015 and Guo et al., 2015). As per our knowledge, this is the first report to use FCN as a tag on the lateral flow biosensors for DNA detection. The FCN-based LFNAB in this research is by far the most sensitive method reported for the rapid detection of DNA sequence on a lateral flow device

without additional signal amplification and the use of conventional fluorophores and QDs. We demonstrated that the biosensor was able to detect a minimum concentration of 0.4 fM DNA. The resulting fluorescent lateral flow assay presents a rapid, low-cost and a very sensitive DNA detection method without the need for target amplification or any expensive instrumentation. The promising properties of the FCN-based LFNAB are reported in the following sections.

2. MATERIALS AND METHODS

2.1 Apparatus

The Biojet BJQ 3000 dispenser, Airjet AJQ 3000 dispenser, Clamshell Laminator and the Guillotine cutting module CM 4000 were purchased from Biodot LTD (Irvine, CA) and used to prepare the lateral flow nucleic acid biosensors. A portable ESE-Quant Lateral Flow Reader (ESE GmbH, Germany) was used to measure the fluorescent intensities of the test zone and control zone of the lateral flow nucleic acid biosensors. A Hitachi HT7700 field transmission electron microscope (TEM; Tokyo, Japan) was used to take images of carbon nanoparticles. Fluorescent spectra of the fluorescent carbon nanoparticle solution were recorded on a F-4500 fluorescence spectrophotometer (Hitachi, Tokyo, Japan). PowerPac^{TM} Basic Power Supply and Mini-Sub Cell GT Cell were purchased from Bio-Rad (Hercules, CA).

2.2 Reagents and materials

Glacial acetic acid, diphosphorus pentoxide, streptavidin, Methane diamine, 1,3 di-amino-propane, hexa methylene diamine, bovine serum albumin (BSA), EDC (N-(3-dimethylaminopropyl)-N′-ethylcarbodiimide hydrochloride), sulfo NHS (*N*-Hydroxysulfosuccinimide sodium salt), MES (2-(*N*-morpholino)ethanesulfonicacid) buffer, Caesin, PVP (Polyvinylpyrrolidone), Tween 20, Ethidium Bromide and Orange-G dye, PBS

(phosphate-buffered saline) buffer, TBS (Tris-buffered saline) buffer, PBST (phosphate-buffered saline with tween-20) were purchased from Sigma-Aldrich (St. Louis, MO). Glass fibers (GFCP000800), cellulose fiber sample pads (CFSP001700), laminated cards (HF000MC100) and nitrocellulose membranes (HFB18004) were purchased from Millipore (Billerica, MA). TAE (Tris base, acetic acid and EDTA) buffer and agarose were purchased from Promega (Madison, WI). 500-50 bp DNA ladder were purchased from Norgen (Ontario, Canada).

All the chemicals used in this study were analytical reagent grade. Solutions were prepared with ultrapure (Z18 MΩ) water from Millipore Milli-Q water purification system (Billerica, MA). All the DNA oligonucleotides used in this study were purchased from Integrated DNA Technologies, Inc. (Coralville, IA) and had the following sequence:

Target DNA: 5′-ATGACCTATGAATTGACAGAC-3′.

Amine-modified detection DNA probe:5′-Amino-GTCTGT CAA-3′.

Biotinylated capture DNA probe: 5′-ATAGGTCAT/Biotin-3′.

Biotinylated control DNA probe: 5′-Biotin/MC6-D/TTGACA GAC-3′.

Non-complementary DNA: 5′-CATTCCAGCAGCTGTTT-3′.

One-base mismatched DNA: ATAACCTATGAATTGACAGAC

Two-base mismatched DNA: ATAATCTATGAATTGACAGAC

2.3 Preparation of fluorescent carbon nanoparticles (FCN) and FCN-DNA Conjugates

FCNs were synthesized as follows using the procedure reported by *Fang et.al* (Fang et al., 2012). one milliliter of glacial acetic acid containing 80 μL of water was added to 2.5 g of P_2O_5 in a 25 mL beaker without stirring. The reaction mixture was quickly foaming because of the

spontaneous heat and gradually cooled down to room temperature. The dark brown mixture was then dispersed in water and centrifuged at 13000 rpm for 10 min to collect the supernatant. One milliliter of FCN solution was then mixed with 9.6 mg of EDC and 5.43 mg of sulfo-NHS in 1.0 mL MES buffer (0.1 M, pH 4.7). The mixture was incubated at room temperature for 30 min. The pH was then adjusted to 7.0 followed by the addition of 2-mercaptoethanol to inactivate the EDC. The amine-modified detection DNA probe was then added to the activated FCNs with a final concentration of 0.1 OD mL^{-1} and incubated for 3 h at room temperature. The conjugates were blocked with 1% BSA for 30 min. A centrifugal filter unit (cutoff: 3K) for concentration and purification of biological solution was used to separate the unbound DNA in conjugation solution. Molecular weight of DNA probe was less than the cutoff value of the filter (3K). Hence any unbound DNA would be removed. The washes were done multiple times and the final eluent was checked with UV- Visible spectrometry to ensure there was no DNA absorption peak. The remained FCN-DNA conjugate in the filter was also examined with UV-Visible spectrometry.

2.4 FTIR Sample Preparation

The FCNs were first extracted from water using ethyl acetate followed by the addition of KBr powder. Then the ethyl acetate was completely vaporized and the solid was kept for drying in a vacuum oven for 12h for the collection of FTIR spectra.

2.5 Preparation of streptavidin-biotin-DNA conjugates

One hundred nanomoles of biotinylated DNA probe (capture DNA probe) was mixed with 2.5 mg mL^{-1} streptavidin and incubated at room temperature for 1 hour. After adding 500 µL PBS to

the mixture, the new solution was centrifuged using a centrifugal filter for 20 minutes at 6000 rpm at 4 ℃ to remove the unbound DNA. The above step was repeated for 3 times. The remaining solution in filter was diluted with PBS and used for dispensing. The same procedure was followed for the preparation of streptavidin-biotin-control DNA probe.

2.6 Preparation of lateral flow nucleic acid biosensor (LFNAB)

A lateral flow nucleic acid biosensor (LFNAB) consists of the following components: sample application pad, conjugate pad, nitrocellulose membrane, and absorbent pad. The sample application pad (17 mm x 30 cm) was made from cellulose fiber (CFSP001700) and soaked in a solution containing 0.25% Triton X-100, 0.05M Tris-HCl and 0.15 M NaCl for one hour, dried and stored at room temperature for further use. The FCN-DNA (detection probe) conjugate solution was dispensed on the glass fiber conjugate pad with Airjet AJQ 3000 dispenser. Streptavidin-biotin-capture DNA probe and streptavidin-biotin-capture control DNA probe solutions were dispensed on the nitrocellulose membrane to form the test and control zones, respectively. After dispensing, the conjugate pad and nitrocellulose membrane were dried at 37^{o}C for 1 hr before assembly. Finally, all the components were assembled onto a plastic adhesive backing (60 mm x 30 cm) using a clamshell laminator. Each part overlapped 2 mm to ensure the solution could migrate through the strip during the assay. Strips with 3 mm width were cut by the Guillotin cutting module CM 4000.

2.7 Sample assay procedure

Sample solutions with different concentrations of target DNA were prepared in the running buffer (PBS + 0.5% BSA). In a typical assay, 100 μL of sample solution was applied onto the sample pad, then the solution migrated toward absorption pad. During the assay process, the solution migrated up by capillary force. The test zone and control zone were evaluated visually under UV light within 20 min. For quantitative measurements, the fluorescent intensities of the test line and control line were recorded by a portable ESE-Quant lateral flow reader.

3. RESULTS AND DISCUSSION

3.1 Preparation of fluorescent carbon nanoparticles (FCNs) and FCN-DNA conjugates

Fluorescent carbon nanoparticles (FCNs) have been considered as an alternative for fluorescent chalcogenide semiconductor nanocrystals (QDs) and used in bioimaging, photo catalysis, and light-emitting services (Fang et al., 2012). The analytical applications of FCNs mainly concentrated on the fluorescent detection of metal ions (Cui et al., 2015 and Guo et al., 2015). There are few reports on biosensors and bioassays (Dai et al., 2014 and Wang et al., 2011). In this study, FCNs were first used as tags to develop a fluorescent lateral flow nucleic acid biosensor for ultrasensitive detection of DNA sequences. FCNs were prepared according to the reported methods with slight modifications (Fang et al., 2012). Transmission electron microscopy (TEM), FT-IR and fluorescent spectra were used to characterize the FCNs. **Figure 1A** shows the typical TEM image of the as-prepared FCNs. One can see the diameter of FCN is around 15 nm and the size distribution is uniform. **Figure 1B** presents the fluorescent emission spectra of a 100-fold diluted FCN solution with an excitation wavelength of 365 nm, a well-defined emission peak with the maxima emission wavelength of 510 nm was obtained. The

fluorescent intensities of the FCN solution increased with the increase of the concentration of FCN (Supporting information(SI), Figure S1). The FTIR spectrum of the FCNs (Figure 1C) has an apparent peak around 3400cm^{-1} indicating the presence of –OH groups and a peak at 1656cm^{-1} indicating the existence of C=O group conjugated with aromatic carbons respectively. A peak at 1627cm^{-1} indicate the presence of conjugated c=c stretching vibration. These data reveal that the synthesized FCNs are rich in carboxylic groups. The amino-modified detection DNA probe was conjugated to the FCN surface by using EDC and NHS coupling reagents (**Figure 1D**). There was no change of the fluorescence intensity of the FCN observed prior to and after DNA conjugation (SI, Figure S2). UV-Visible spectrum was used to characterize the FCN-DNA conjugates. There are two absorption peaks at 260 nm and 300 nm in the UV-Visible spectrum of FCN (SI, Figure S3). The absorption peak at 260 nm is overlapped with the absorption peak of DNA. It was found that the absorption peak intensity at 260 nm increased significantly, indicating the DNA probes were conjugated to FCN.

An agarose gel electrophoresis was used to further confirm the formation of carbon nanoparticle-DNA conjugates. Fig. S4 presents the typical agarose electrophoresis image. One can see that the formed duplex DNA in lane 2 (without FCN) had greater mobility than that in lane 3, in which the duplex DNA were formed on the FCN surface. Such mobility difference was caused by the formation of FCN-duplex DNA complexes, which had larger mass than the free duplex DNA (lane 2) and slow down its movement in the agarose gel. Control experiments were performed by adding pure FCNs (without conjugation with the detection DNA probe) in lane 4 and the mixture of FCNs, detection DNA probe and complementary DNA in lane 5. There is no band observed in lane 4, and a bright band at the same position as in lane 2 is shown in lane 5.

The above results confirmed that the detection DNA probes were conjugated with FCNs successfully.

We compared the performances of FCN-DNA conjugates with and without spacers. Methane diamine, 1,3 di-amino-propane, hexa methylene diamine were used as spacers to prepare the FCN-DNA conjugates. It was found that the fluorescence intensities of the test line with FCN-DNA-spacer was much lower than that FCN-DNA without spacer (SI, Figure S5). The decrease of fluorescence intensity may be caused by the small size of FCN. The addition of spacers on the FCN surface decreased the DNA probes immobilized on FCN surface and reduced the DNA hybridization efficiency during the lateral flow assay, resulting less FCNs were captured on the test line and a decrease of fluorescence intensity. Therefore, FCN-DNA conjugates were prepared without adding the spacers in the following experiments. The formed FCN-DNA conjugate was dispersed in the eluent buffer and used to prepare the lateral flow nucleic acid biosensors (LFNABs).

3.2 Principle of DNA detection with the FCN-based LFNAB

The FCN-based LFNAB configuration is illustrated in **Figure 2A**. A pair of DNA probes, named detection DNA probe and capture DNA probe, was used to prepare the LFNAB. The capture DNA probe and detection DNA probe are complementary with target DNA at different portions. The detection DNA probe was conjugated with FCN and the FCN-DNA conjugates were dispensed on the conjugate pad of the LFNAB. Biotin-modified capture DNA probe was first reacted with streptavidin and the resulting streptavidin-biotin-capture DNA complexes were dispensed on test zone of the LFNAB to form a test line. The third DNA probe, named control DNA probe, which is fully complementary with the detection DNA probe, was immobilized on the control zone to form a control line. In a typical assay, the sample solution containing desired

concentrations of target DNA was applied to the sample pad. The solution migrated along the strip by capillary force and FCN-detection DNA probe-target DNA complexes were formed due to the DNA hybridization reactions between the target DNAs and the detection DNA probes. Upon reaching the test-zone, it forms a sandwich-type complex because of the second DNA hybridization reaction between the capture DNA and target DNA (**Figure 2A**). The excess of the FCN-DNA conjugates continues to move until it reaches the control zone where it was captured by the control DNA probe. The control line is used to confirm if the LFNAB is working properly. In the absence of the target DNA, there is no sandwich-type complex formed on the test zone and only the FCN-detection DNA-control DNA complexes formed on the control zone. The amount of the captured FCNs on the test zone is proportional to the target DNA concentration in the sample solution and can be used to quantify the target DNA concentration qualitatively and quantitatively. Qualitative analysis can be performed by observing the test line and control line under a UV light (**Figure 2B**); In the presence of target DNA, a test band and a control band will show on the nitrocellulose membrane (**Figure 2B**, middle), and only the control band will appear in the absence target DNA (**Figure 2B**, Left). There is no band appeared if the LFNAB is not working properly (**Figure 2B, right**). Quantitative analysis can be done by reading the fluorescent intensities of the test zone using a portable ESE-Quant lateral flow reader (**Figure 2C**). In the presence of target DNA, two peaks depicting the responses from the test zone and the control zone will be observed (**Figure 2C**, middle). Only one peak from the control zone will be detected in the absence of target DNA (**Figure 2C**, left), as there was no FCN captured on the test zone. No peak from both the test zone and the control zone indicates the LFNAB is not working properly (**Figure 2C**, right).

Figure 3A presents the typical photo images of the LFNABs in the presence of 0 pM target DNA (control test), 1.0 pM target DNA, 50 nM noncomplementary DNA and the mixture of 50 nM noncomplementary DNA and 1.0 pM target DNA. The images were taken under an UV light with a wavelength of 365 nm. Two bright bands were observed in the presence of 1.0 pM target DNA, and only one band (control line) was observed in the absence of target DNA and presence of excess of noncomplementary DNA. The intensities of test bands in the presence of 1.0 pM target DNA and the mixture of 1.0 pM target DNA and 50 nM noncomplementary DNA are almost equal, indicating the presence of excess of noncomplementary DNA does not affect the signal of target DNA (SI, Figure S6). The fluorescent intensities of the bands were recorded with a portable ESE-Quant lateral flow reader and the responses are shown on **Figure 3B** (no target DNA) and **Figure 3C** (1 pM target DNA). Well-defined peaks were observed, and the peak areas were proportional to the captured FCNs in the control line (left side) and test line (right side). It was also noticed that there was a small peak observed in the test zone of the biosensor in the absence of target DNA (**Figure 3B**), which was caused by the nonspecific adsorption of the FCN-detection DNA conjugates on the membrane. To reduce such nonspecific adsorption, the nitrocellulose membrane was blocked for an hour prior to the dispensing of the streptavidin-biotin-capture DNA and streptavidin-biotin-control DNA solutions by using a buffer containing 0.01% BSA, 0.02% PVP, 0.005% Casein, 1X TBS and 0.002% Tween-20. **Figure 3D** presents the effect of blocking step on the signal-to-noise (S/N) of the assay. One can see the S/N ratio of the assay with the blocking step is 2.5 times higher than that of the assay without blocking step.

3.3 Optimization of Experimental Parameters

To acquire the sensitive DNA detection using the FCN-based LFNAB, different experimental parameters including the running buffers, the concentration of amino-modified detection DNA probe used in the preparation of FCN-DNA conjugates, the volume of the conjugate dispensed on the conjugate pad and the dispensing cycles of the capture DNA probes on the test-zone were optimized.

The effect of the running buffers is considered as one of the most important parameters in the optimization of the lateral flow assays. Appropriate buffers would minimize the nonspecific adsorption and increase the sensitivity and reproducibility of the assay. We compared the performances of FCN-based LFNAB tests with different running buffers including PBS+1% Tween, PBS + 1% BSA, PBS + 0.5% BSA, PBS + 0.1% BSA and PBST+0.5% BSA. As shown in the **Figure 4A**, the highest S/N ratio was obtained by using PBS+0.5% BSA, which was used as the running buffer for all the assays.

In the current study, the FCN-detection DNA probe conjugates were dispensed on the glass fiber. The fluorescent intensities of test zone and control zone depended on the amount of FCN-detection DNA probe conjugate captured on the zones, which in turn correspond to the amount of conjugates dispensed on the conjugate pad. The amount of FCN-detection DNA probe conjugates on the conjugate pad was controlled by the dispensing volume of the conjugate solution. **Figure 4B** presents the histogram of the S/N ratio for 1.0 pM target DNA test with the different amount of FCN-detection DNA probe conjugate loaded conjugate pads. The S/N ratio of the assay increased up to 6 μL on the conjugate pad, which was used as the optimal volume of the FCN-detection DNA probe conjugates for most of the experiments. The further increase of the dispensing volume of FCN-DNA conjugates led to a decrease in the S/N ratio due to an increasingly nonspecific adsorption.

In addition, the amount of detection DNA probe on the FCN surface would affect the responses of the LFNABs. We studied the effect of DNA probe concentration during the preparation of FCN-detection DNA probe conjugates on the S/N ratio of the LFNAB (**Figure 4C**). One can see that the S/N ratio increases upon raising the DNA concentration in the conjugate solution from 0.05 OD/mL to 0.1OD/mL, and then it starts to level off till 0.3 OD/mL; the further increase of the DNA concentration led to a decrease in the S/N ratio. The decrease of S/N at high concentration of detection DNA probe would be caused by the number of DNA probes on the FCN surface. More DNA probes were immobilized on the FCN surface and less FCNs would be captured on the test zone. Therefore, a DNA probe concentration of 0.1 OD/mL in the conjugate solution was used to prepare the FCN-detection DNA probe conjugates for the following experiments.

Another factor to affect the sensitivity and reproducibility of the LFNAB test is the amount of capture DNA probes dispensed on the test-zone. To obtain the best S/N ratio, increasing amounts of biotin-streptavidin capture DNA probe were used to prepare the test line of the LFNAB. This was done by increasing the number of dispensing cycles. As shown in **Figure 4D**, five times dispensing of the capture DNA probe was giving the highest S/N ratio. This optimized condition was used in further assays.

3.4 Analytical Performance

Under optimized experimental conditions, the performance of the FCN-LFNAB was tested in the presence of different target DNA concentrations. The captured FCNs on the test line would be observed visually by using a UV lamp, and quantified by measuring the fluorescent intensity of the test line with the portable fluorescent reader. The test-line was quite visible even in the

presence of 0.05 pM target DNA, which could be estimated as a threshold for the qualitative detection of the target DNA. A series of well-defined peaks were observed and the intensity increased with increasing target DNA concentration. The resulting calibration curve of the logarithm of target DNA concentration versus the fluorescent intensity was linear over a range of 1.0 fM to 10 nM (Fig.5) with a detection limit of 0.4 fM. The assay time was around 20 min. Table 1 shows the detection limits of the reported lateral flow DNA/microRNA assays based on different labels and signal amplification methods. The DL of FCN-based LFNAB in this report is 4 to 6 orders lower than that of GNP-based LFNAB without signal amplification, and is comparable with that of LFNAB with additional signal amplification. Compared with references [Liu et al. 2009; Liu et al. 2013 and Mao et al. 2009] in Table 1, the advantages of the proposed method in this report include: (1) the preparation of FCNs was very convenient; (2) the low detection limit was obtained without complex procedures and additional signal amplification; (3) the cost of FCNs is much lower than that of GNP. Selectivity of FCN-based LFNAB was studied by testing the responses of one-base mismatched DNA, two-base mismatched DNA and complementary target DNA at the same concentration level. It was found that similar responses were obtained from the one-base mismatched DNA and complementary DNA, and the response of two-mismatched DNA was much lower than that of complementary DNA. (SI, Figure S7) The results indicated the FCN-based LFNAB was able to differentiate two-base mismatched DNA from the target DNA. Reproducibility of FCN-based LFNAB was tested in the absence and presence of 0.5 pM and 1.0 nM concentrations of target DNA. Samples were tested for 6 times with the same concentrations and the fluorescence intensities of the LFNAB test line were measured. The relative standard deviation for 0 nM, 0.5 pM and 1.0 nM was 3.9%, 7.2% and 4.7%, respectively, indicating a very good reproducibility.

The anti-interference ability and applicability of testing DNA in real samples of the proposed method were studied by testing target DNA in spiked human plasma samples. The plasma samples were then diluted to 2.5% with running buffer. The results as shown in Figure S8 (SI) indicates the proposed method has excellent anti-interference ability. The recoveries of 98% and 101% were obtained for 1 nM and 0.5 pM target, respectively, indicating the potential of the developed assay for future clinical applications.

4. Conclusion

5. Fluorescent carbon nanoparticle was first used as a tag to develop a lateral flow nucleic acid biosensor for ultrasensitive and quantitative detection of nucleic acid samples. Under optimal conditions, the FCN-based LFNAB was capable of detecting minimum 0.4 fM target DNA without complex operations and additional signal amplification. Moreover, the use of fluorescent carbon nanoparticles eliminates the tedious synthesis procedures required for the preparation of fluorescent nanoparticles. Further work will aim to study the multiplex capability of the fluorescence carbon nanoparticles with different diameters and explore its applications in immunoassay. The FCN-based LFNAB in this report shows great promise for rapid, low-cost and sensitive detection of nucleic acids, particularly in limited resource settings.

ACKNOWLEDGMENT

This research was support by the National Institute of Health, Centers of Biomedical Research Excellence (NIH, COBRE, Grant number: 1P20 GM109024-01A1). Its contents are solely the responsibility of the authors and do not necessarily represent the official views of the NIH.

REFERENCES

1. Ang, G. Y., Yu, C. Y., Yean, C. Y., 2012. Biosens. Bioelectron. 38 (1), 151-156.
2. Baeumner, A.J., Pretz, J., Fang, S., 2004. Anal. Chem. 76, 888-894.
3. Cao, L., Sahu, S., Anilkumar, P., Bunker, C. E., Xu, J., Fernando, K. A. S., Wang, P., Guliants, E. A., Tackett, K. N., Sun, Y., 2011. J. Am. Chem. Soc. 133, 4754–4757.
4. Cao, L., Wang, X., Meziani, M. J., Lu, F., Wang, H., Luo, P. G., Lin, Y., Harruff, B. A., Veca, L. M., Murray, D., Xie, S., Sun, Y., 2007. J. Am. Chem. Soc. 129, 11318–11319.
5. Carter, D. J., Cary, R. B., 2007. Nucleic Acids Res. 35 (10), e74.
6. Corstjens, P. L. A. M., Zuiderwijk, M., Nilsson, M., Feindt, H., Niedbala, R. S., Tanke, H. J., 2003. Anal. Biochem. 312, 191-200.
7. Cui, X., Zhu, L., Wu, J., Hou, Y., Wang, P., Wang, Z., Yang, M., 2015. Biosens. Bioelectron. 63, 506–512.
8. Dai, H., Shi, Y., Wang, Y., Sun, Y., Hu, J., Ni, P., Li, Z., 2014. Sens. Actuators, B. 202, 201–208.
9. Fang, Y., Guo, S., Li, D., Zhu, C., Ren, W., Dong, S., Wang, E., 2012. ACS Nano. 6 (1), 400-409.
10. Fang, Z., Huang, J., Lie, P., Xiao, Z., Ouyang, C., Wu, Q., Wu, Y., Liu, G., Zeng, L., 2010. Chem. Commun. 46, 9043-9045.
11. Gao, X., Xu, H., Baloda, M., Gurung, A. S., Wang, T., Zhang, X., Liu G., 2014. Biosens. Bioelectron. 54, 578–584.
12. Ge, X., Asiri, A. M., Du, D., Wen, W., Wang, S., Lin, Y., 2014. TrAC. Trends Anal. Chem. 58, 31–39.

13. Guo, Y., Zhang, L., Zhang, S., Yang, Y., Chen, X., Zhang, M., 2015. Biosens. Bioelectron. 63, 61–71.
14. He, Y., Zeng, K., Gurung, A., Baloda, M., Xu, H., Zhang. X., Liu, G., 2010. Anal. Chem. 82 (17), 7169–7177.
15. He, Y., Zeng, K., Zhang, X., Gurung, A. S., Baloda, M., Xu, H., Liu, G., 2010. Electrochem. Commun. 12, 985-988.
16. He, Y., Zhang, S., Zhang, X., Baloda, M., Gurung, A. S., Xu, H., Zhang, X., Liu, G., 2011. Biosens. Bioelectron. 26(5), 2018-2024.
17. He, Y., Zhang, X., Zeng, K., Zhang, X., Baloda, M., Gurung, A. S., Liu G., 2011. Biosens. Bioelectron. 26(11), 4464-4470.
18. Jaroenram, W., Kiatpathomchai, W., Flegel, T. W., 2009. Mol. Cell. Probe. 23 (2), 65-70.
19. Kim, S. E., Ahn, K. Y., Park, J. S., Kim, K. R., Lee, K. E., Han, S. S., Lee, J., 2011. Anal. Chem. 83, 5834-5835.
20. Li, H., He, X., Kang, Z., Huang, H., Liu, Y., Liu, J., Lian, S., Tsang, C. H., Yang, X., Lee, S. T., 2010. Angew. Chem. Int. Ed. 49, 4430–4434.
21. Li, Z., Wang, Y., Wang, J., Tang, Z., Pounds, J. G, Lin, Y., 2010. Anal. Chem. 82, 7008-7014.
22. Lie, P., Liu, J., Fang, Z., Dun, B., Zeng, L., 2012. Chem. Commun. 48 (2), 236-238.
23. Liu, G., Mao, X., Phillips, J. A., Xu, H., Tan, W., Zeng, L., 2009. Anal. Chem. 81 (24), 10013-10018.
24. Liu, J., Chen, L., Lie, P., Dun, B., Zeng, L., 2013. Chem. Commun. 49 (45), 5165-5167.
25. Mao, X., Ma, Y., Zhang, A., Zhang. L., Zeng, L., Liu, G., 2009. Anal. Chem. 81 (4), 1660–1668.
26. Mao, X., Wang, W., Du, T. E., 2013. Talanta. 114, 248-253.
27. Mao, X., Xu, H., Zeng, Q., Zeng, L., Liu, G., 2009. Chem. Commun. 21, 3065-3067.
28. Mens, P., de Bes, H., Sondo, P., Laochan, N., Keereecharoen, L., van Amerongen, A., Flint, J., Sak, J., Proux, S., 2012. J. Clin. Microbiol. 50 (11), 3520-3525.
29. Qiu, W., Xu, H., Takalkar, S., Gurung, A. S., Liu, B., Zheng, Y., Guo, Z., Baloda, M., Baryeh, K., Liu, G., 2015. Biosens. Bioelectron. 64, 367-372.
30. Sajid, M., Kawde, A., Daub, M., 2015. Journal of Saudi Chemical Society. 19(6), 689-705.
31. Shipp, G., 2006. Biotechnol Healthc. 3(2), 35-36, 38-40.
32. Wang, F., Chen, Y., Liu, C., Ma, D., 2011. Chem. Commun. 47, 3502–3504.
33. Wang, Y., Bao, L., Liu, Z., Pang, D., 2011. Anal. Chem. 83, 8130–8137.
34. Wang, Y., Nugen, S. R., 2013. Biomed. Microdev. 15, 751-758.
35. Weller, M.G., 2000. Fresenius J Anal Chem. 366(6-7), 635-645.
36. Xu, H., Chen, J., Birrenkott, J., Zhao, J. X., Takalkar, S., Baryeh, K., Liu, G., 2014. Anal. Chem. 86 (15), 7351–7359.
37. Xu, H., Mao, X., Zeng, Q., Wang, S., Kawde, A., Liu, G., 2009. Anal. Chem. 81 (2), 669–675.
38. Xu, Y., Liu, Y., Wu, Y., Xia, X., Liao, Y., Li, Q., 2014. Anal. Chem. 86, 5611-5614.
39. Yang, S., Cao, L., Luo, P. G., Lu, F., Wang, X., Wang, H., Meziani, M. J., Liu, Y., Qi, G., Sun, Y. P., 2009. J. Am. Chem. Soc. 131, 11308–11309.
40. Zheng, D., Zou, R., Lou, X., 2012. Anal. Chem. 84, 3554-3560.

Captions of Figures and Table

Figure 1. **(A)** Typical TEM image of fluorescent carbon nanoparticles; **(B)** Fluorescent emission spectra of carbon nanoparticle solution, excitation wavelength: 346 nm; (C) FTIR spectrum of fluorescent carbon nanoparticles; **(D)** Schematic illustration of preparing the FCN-DNA conjugates.

Figure 2. (A) Schematic illustration of the configuration and measurement principle of the fluorescent carbon nanoparticle based lateral flow nucleic acid biosensor; (**B**) principle of qualitative detection of DNA on the fluorescent carbon nanoparticle based lateral flow nucleic acid biosensor; (**C**) principle of quantitative detection of DNA with a portable ESE-Quant lateral flow reader. Left: control (in the absence of target DNA); Middle: Sample (in the presence of target DNA); Right: invalid test.

Figure 3. (A) Typical photo images of FCN-based LFNABs after applying 0 nM target DNA, 1.0 pM target DNA, 50 nM noncomplementary DNA and the mixture of 1.0 pM target DNA and 50 nM target DNA. The images were recorded under a UV lamp; (B) The fluorescent responses of the test line and control line of the FCN-based LFNAB in the absence of target DNA. Peak on the left: fluorescent signal from the control line; peak one the right side: fluorescent signal from the test line; (C) The fluorescent responses of the test line and control line of the FCN-based LFNAB in the presence of target 1.0 pM DNA; (D) The histogram of the S/N ratio of the FCN-LFNAB without and with blocking step. Target DNA concentration: 1.0 pM.

Figure 4. (**A**) Effect of running buffers on the S/N ratio of the FCN-based LFNAB; (**B**) Effect of the volume of FCN-DNA conjugate used on the S/N ratio of FCN-based LFNAB; (**C**) Effect of the concentration of detection DNA probe conjugated to FCN on the S/N ratio of FCN-based LFNAB; (D) Effect of the dispensing times of capture DNA on the S/N ratio of FCN-based LFNAB. Target DNA concentration: 1 pM;

Figure 5. Typical photo images and calibration curve of the FCN-based LFNAB with different concentrations of target DNA under the optimal experimental conditions. Error bars represent standard deviation, n =6.

Table 1. Comparision of the detection limits of different lateral flow DNA assays. * In order to maintain uniformity in the units and make it easy for comparision, the detection limits which

were reported in moles have been converted into molarities in the bracket. The moles were divided by the volume used in the references to get their respective molarities.

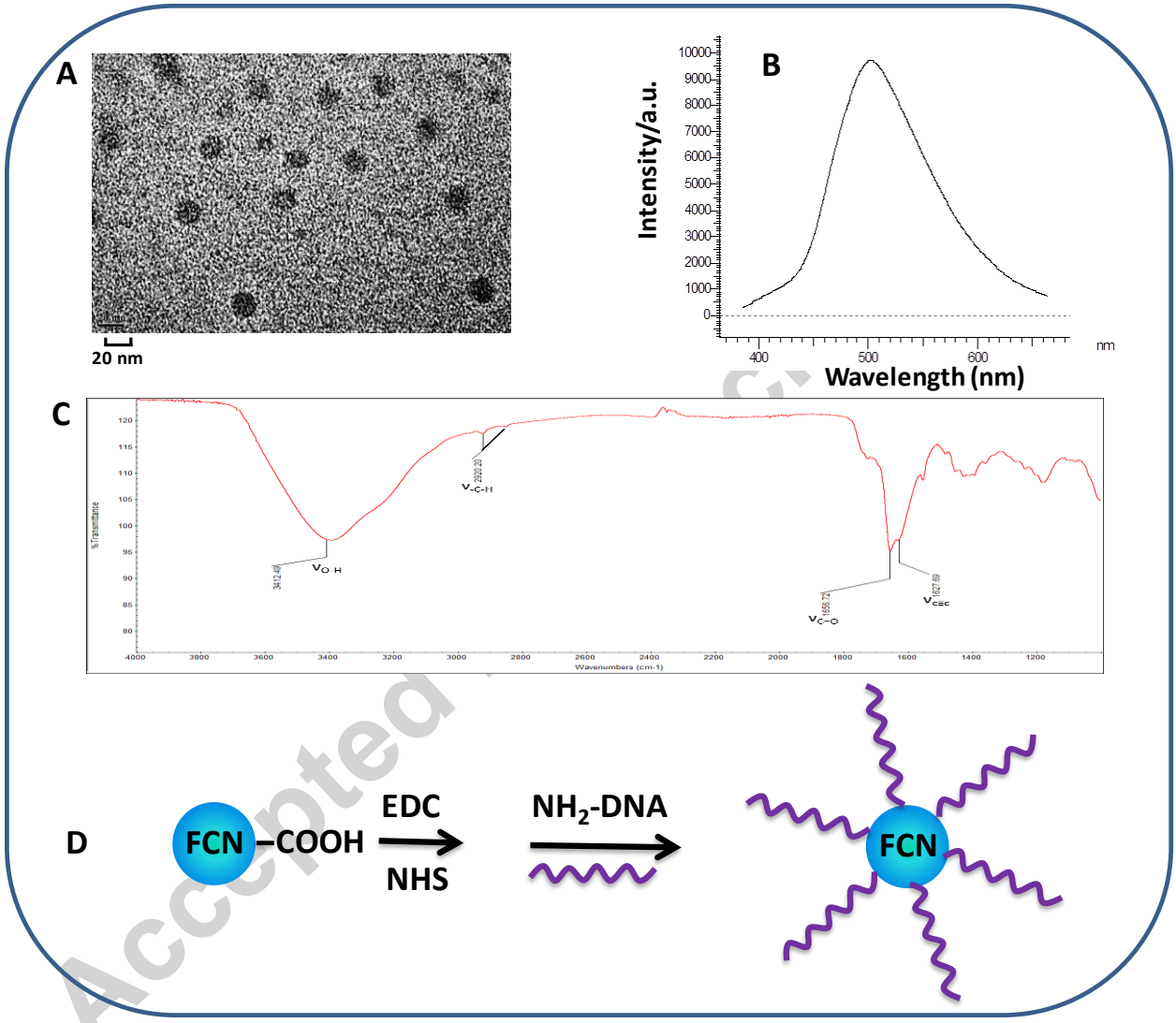

Figure 2

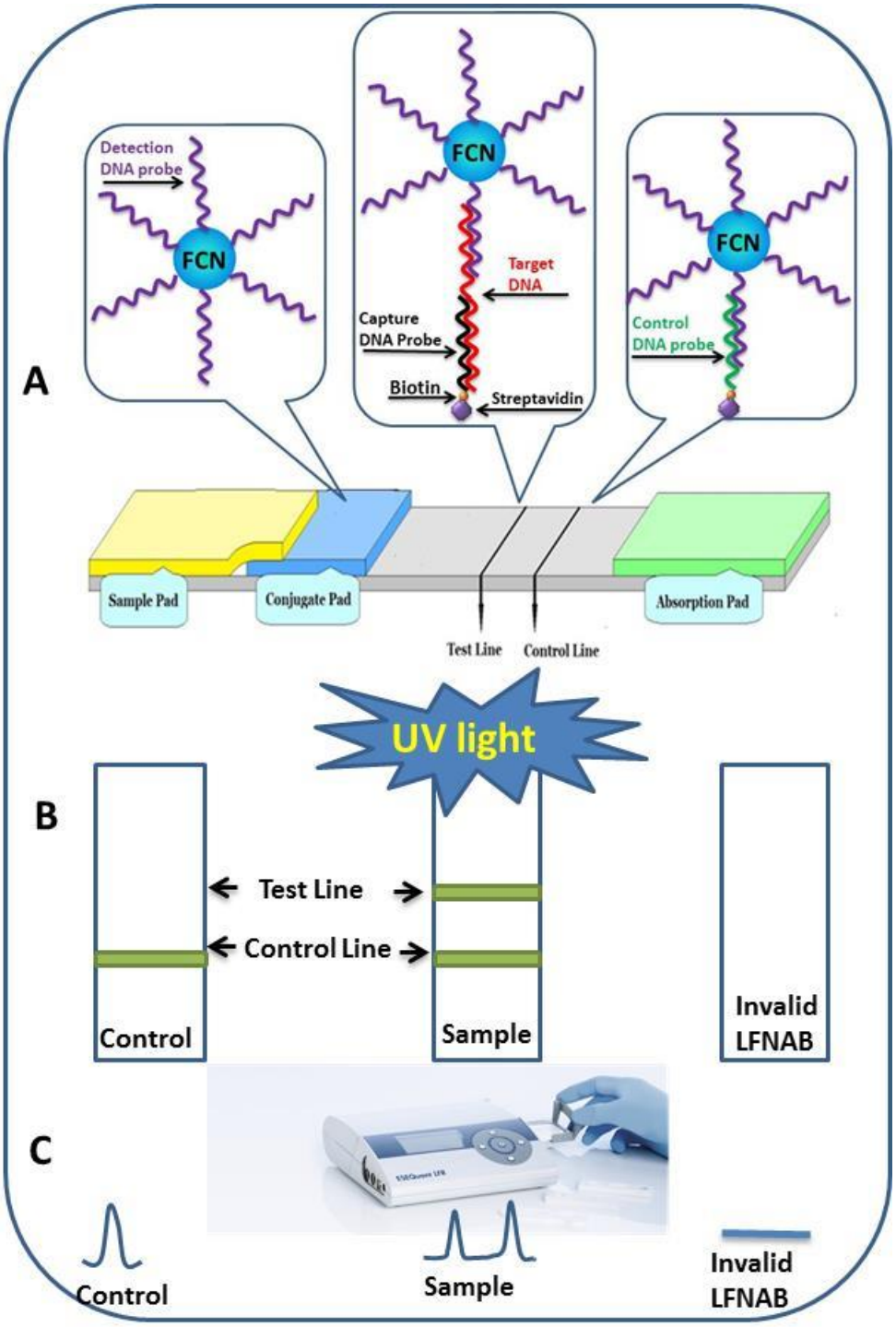
A
Detection DNA probe
FCN
FCN
Target DNA
Capture DNA Probe
Biotin
Streptavidin
FCN
Control DNA probe
Sample Pad
Conjugate Pad
Absorption Pad
Test Line
Control Line
B
UV light
Test Line
Control Line
Control
Sample
Invalid LFNAB
C
Control
Sample
Invalid LFNAB

Figure 3

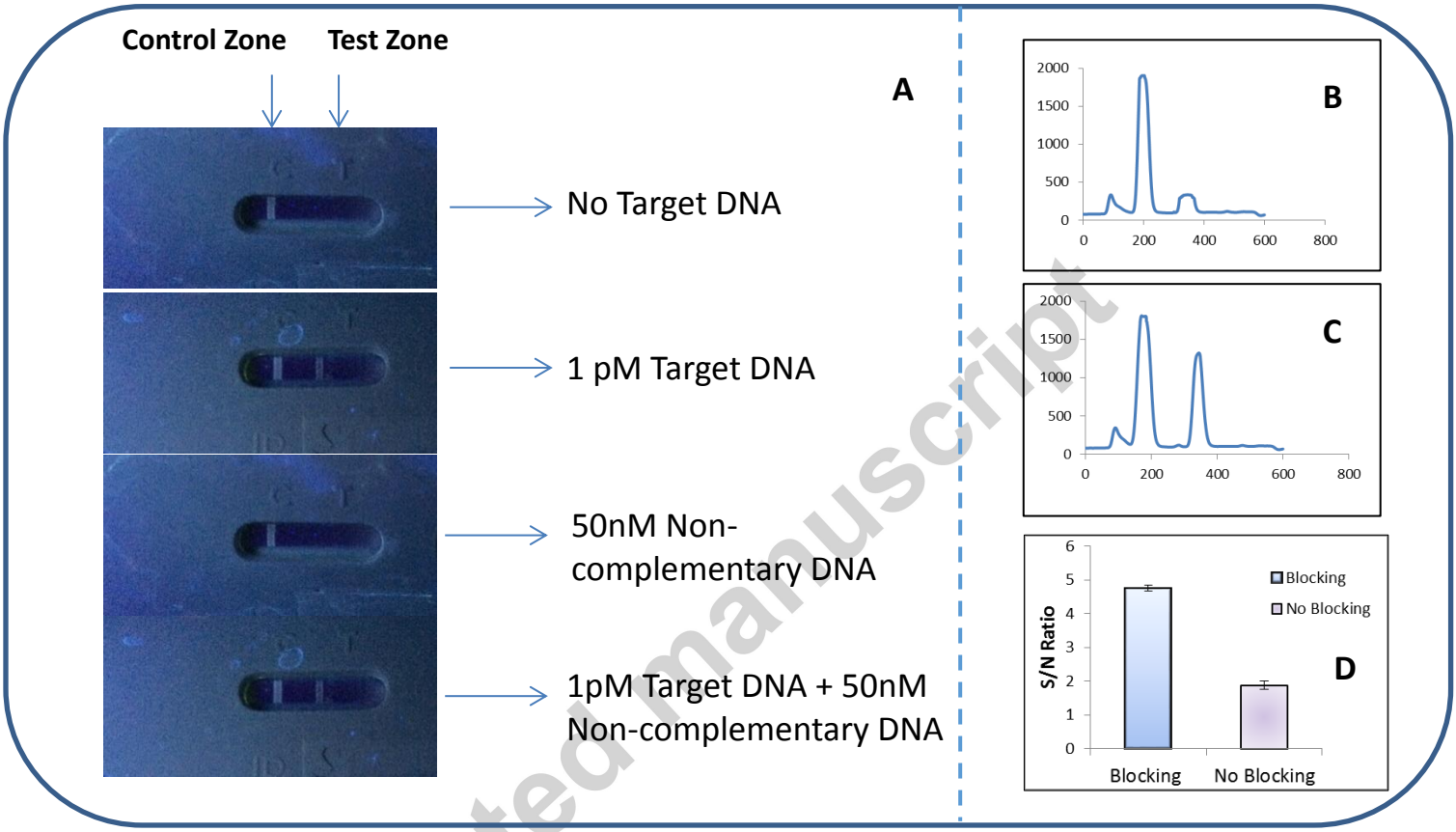

Figure 4

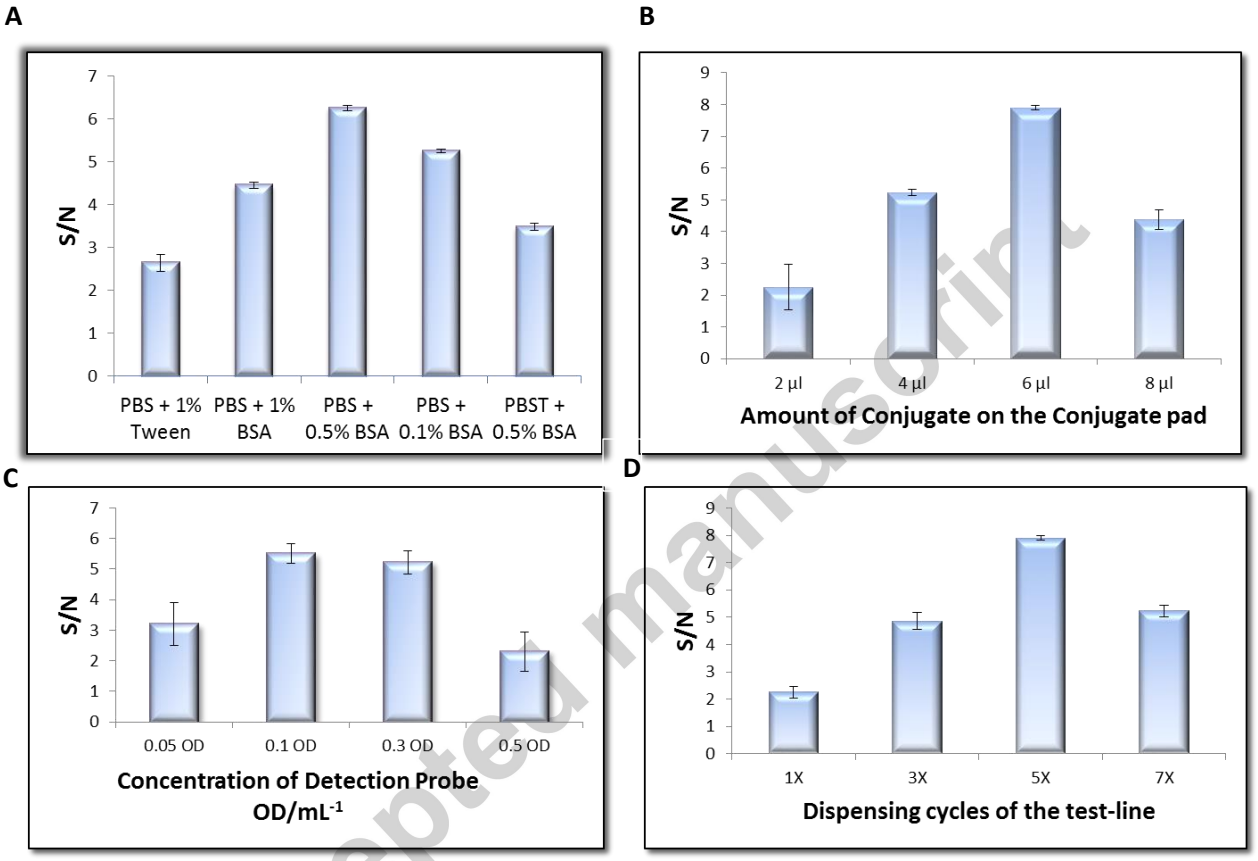

Figure 5

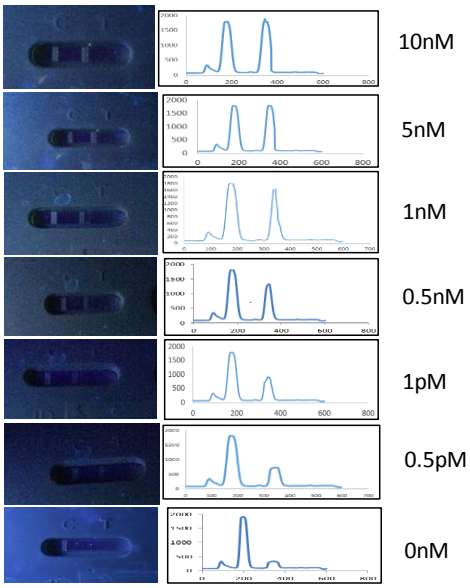

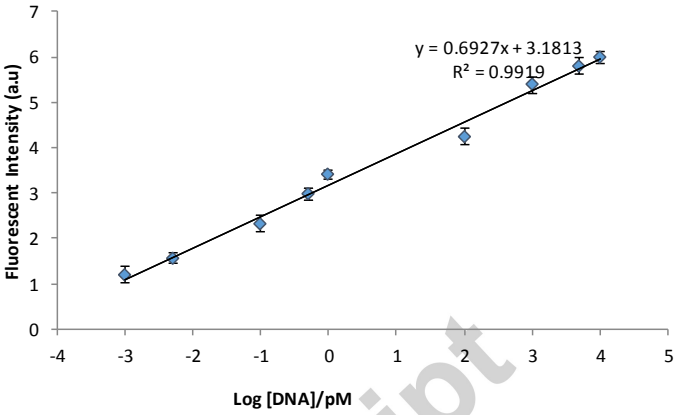

Table 1

Detection Method	Detection Limit	Reference
Fluorescent DNA Probe based lateral flow assay	10-100 copies plasmid DNA / μL	Xu et al. (2014)
Fluorescent dye-doped Nanoparticle based lateral flow assay	0.066 fmols (1 pM)*	Wang et al. (2013)
UPT (Upcoverting Phosphor Technology) particle based lateral flow assay	0.1 fmol (1 pM)*	Corstjens et al. (2003)
Dye entrapping liposomal nanovesicle based universal biosensor	1 nM	Baeumner et al. (2004)
Copper dependent DNA-cleaving DNAzyme and Gold nanoparticle based lateral flow assay	10 nM	Fang et al. (2010)
Blue dye doped latex bead based lateral flow strip	3.75 fmol (28.85 pM)*	Mao et al (2013)
DNA-Gold nanoparticle based lateral flow biosensor	60 pM	Gao et al. (2014)
Molecular beacon functionalized Gold nanoparticle based lateral flow assay	50 pM	Mao et al. (2009)
DNA-Carbon nanotube based lateral flow biosensor	40 pM	Qiu et al (2015)
Gold nanoparticle- Horseradish Peroxidase dual label based lateral flow biosensor	1.25 fM	Mao et al. (2009)
ISDPR (Isothermal Strand Displacement Polymerase Reaction) and Gold nanoparticle based lateral flow assay	0.01 fM	Lie et al. (2012)
Fluorescent Carbon nanoparticle based lateral flow biosensor (No signal amplification)	0.4 fM	Present Work